Design of antitumor drugs targeting c-Kit receptor by a new mixed ligand-structure based method

Annamaria Martorana, Antonino Lauria*

Dipartimento di Scienze e Tecnologie Biologiche Chimiche e Farmaceutiche "STEBICEF" – University of Palermo, Viale delle Scienze – Ed. 17 -90128 Palermo, Italy.
* Correspondence: antonino.lauria@unipa.it; Tel. +39 091238-96818

Abstract: An important challenge, in the medicinal chemistry field, is the research of novel forceful drugs to overcome tumor-acquired resistance. The c-Kit tyrosine kinase receptor (TKR) represents a suitable target for the carcinogenesis control of gastro-intestinal stromal (GIST), leukemia, and mastocytosis tumors; nevertheless, several hotspot mutations of the protein limit the efficacy of a few clinical administered TKRs inhibitors. In this study, a new *in silico* protocol based on ligand and structure-based combined method is proposed, with the aim to identify a set of new c-Kit inhibitors able to complex c-Kit mutated proteins. A recent and freely available web-server DRUDIT is used for the ligand-based method. The protocol application allows for identifying a new generation of potential TKR inhibitors, which, *in silico*, complex the V654A and T670I mutated proteins and potentially overcome resistant mutations (D816H). The structure-based analysis is performed by Induced Fit Docking (IFD) studies. The comparison between the explored ligands and well-known drugs highlights the possibility to overcome tumor-acquired resistance. The best-selected structures (630705 and SML1348) provide valuable binding affinities with the mutated c-Kit forms (respectively T670I and V654A).

Keywords: c-Kit; drug resistance; molecular docking; *in silico* protocols; DRUDIT web-server

1. Introduction

Targeted treatment is one of the most important and efficacious therapeutic approaches in the cure of cancer. The inhibition of a specific target inserted in the carcinogenic pathways and overexpressed in the tumor district enhances the effectiveness

of a drug, and therefore significantly reduces the side effects of healthy and rapidly replicating tissues. The targeted therapy is characterized by a personalized medicine profile since the treatment is chosen not only according to the site of tumor development but also in relation to its molecular characteristics, which may be different from patient to patient. The proteins that regulate proliferation, differentiation, apoptosis, and cellular invasiveness are at the basis of the transformation of healthy cells into neoplastic ones, and, for this reason, they represent the selective targets of this therapeutic approach [1-4].

Great efforts by the scientific community are recently focused on the research of new drugs with a specific activity on gatekeeper targets, for the treatment of both most recurrent neoplasms, such as the breast, colorectal and lung cancer, and less frequent tumors, such as the carcinoma of the kidney. In this contest, the family of tyrosine kinases receptors (TKRs), plays a crucial role in the processes of cancer growth, since their activities are of primary importance in tumor phenotype maintenance and, at the same time, modulate several functions in the tumor microenvironment [5,6]. The TKRs are membrane receptor proteins with intracellular kinase activity. The binding of a specific ligand to the extracellular domain, usually followed by proteins dimerization, transduces the signal to the intracellular region of kinase, with the consequent change of the catalytic binding site from the inactive to active conformation. The phosphorylation of tyrosine residues triggers the cascade signaling until gene transcriptions. The gene mutations of TKRs affect the kinase activity, and potentially lead to the constitutive activation of the receptors, in absence of their endogen ligands. A deregulated tyrosine kinase activity modifies the physiological balance among cell proliferation, survival, differentiation, and apoptosis processes. This condition can promote neoplastic transformation and contributes to sustaining the malignant phenotype. Chronic activation of several TKRs for growth factors and cytokines is a common marker of different types of human cancers [7]. Experimental data show that tumor cells are often "addicted" to TKR activities since their inhibition severely impairs the proliferation and survival of tumor cells [8].

Based on these features, several TKRs, (such as ABL1, BCR-ABL, BRAF, CRAF, EGFR, FLT3, MET, VEGFR-1, VEGFR-2, RET, PDGFR, and c-KIT), could be identified as key biological targets in anticancer therapeutic protocols. In this work, we focus on several gains of function point mutations of the receptor c-Kit involved in the abnormal cell expression of different proliferating diseases, i.e. gastrointestinal stromal tumor (GIST), leukemia and mastocytosis [9-11].

c-Kit is a member of the Type III transmembrane TKRs subfamily, including FMS, Flt-3, PDGFRα, and β receptors. The activation of c-Kit is generally promoted by the Stem Cell Factor (SCF), a cytokine protein with a crucial role in melanogenesis and hematopoiesis. This TKR is characterized by five extracellular immunoglobulin-like domains, a single transmembrane helix, an autoinhibitory juxtamembrane region (JMR), and a cytoplasmic (proximal and distal) kinase domain (KD), that is split by a kinase insertion domain (KID) [12]. The activated c-Kit kinase conformation is characterized by a catalytic triad of amino acids, the DFG-motif (D810, F811, G812), which is immediately before the A-loop (included in the distal KD), whereby the two amino acids aspartic acid and phenylalanine are oriented towards the proximal KD in the ATP binding pocket (DFG-in). Whereas, in the inactivated conformation, the DFG-motif is distant from the binding site (DFG-out).

The c-Kit JMR is a regulatory region, with an autoinhibitory function. JMR forms a β hairpin loop that inserts into the kinase ATP binding site, interfering with the DFG-motif and the A-loop in the protein activated conformation.

In cancer cells, the constitutive activation of the c-Kit TKR shifts the equilibrium between DFG-out and DFG-in conformations in favour of the open activated form, with the admission of ATP in the binding pocket and the increase of phosphorylation of the tyrosine kinase domain. The subsequent intracellular signaling cascade leads to abnormal tissue proliferation. The clinical administration of TKRs inhibitor *imatinib*, in first-line treatment, turns off c-Kit over-activity. Competing with the ATP binding pocket, it locks c-Kit in an auto-inhibitory conformation [12]. Unfortunately, numerous hotspot mutations in the different domains of c-Kit display acquired resistance to the systematic therapy, with the protein insensitive to *imatinib*. The second-line therapy is provided by several kinase inhibitors, such as *sorafenib*, *sunitinib*, that exhibit efficacy, especially, when c-Kit is mutated into the ATP-binding pocket (V654A and gatekeeper mutant T670I) [13, 14]; however, these drugs are ineffective to many of the mutations detected in the activation loop [15-17]. Even *regorafenib*, approved in the third-line treatment of patients resistant and intolerant to *imatinib* and *sunitinib*, is moderately active against c-Kit secondary mutations, (D816H/V) [14]. With this regard, this work aims to explore new forceful c-Kit TKR inhibitors, proposing a novel *in silico* protocol built on a ligand and structure-based combined method, to suitable inhibit the V654A and T670I mutated proteins and overcome more resistant mutations (D816H).

2. Results and discussion

2.1. Amino acids maps analysis at ATP binding site

The PDB ID 3G0E [19] is selected in order to study the interactions of known inhibitors of c-Kit, reported in Figure 1, with the wild type (WT) and mutated protein forms. 3G0E is the crystallographic representation of c-Kit kinase domain (x-Ray diffraction, 1.6 Å) in complex with *sunitinib* at ATP binding site, in a DFG-conformation out-like and αC-helix conformation out, (Figure 2).

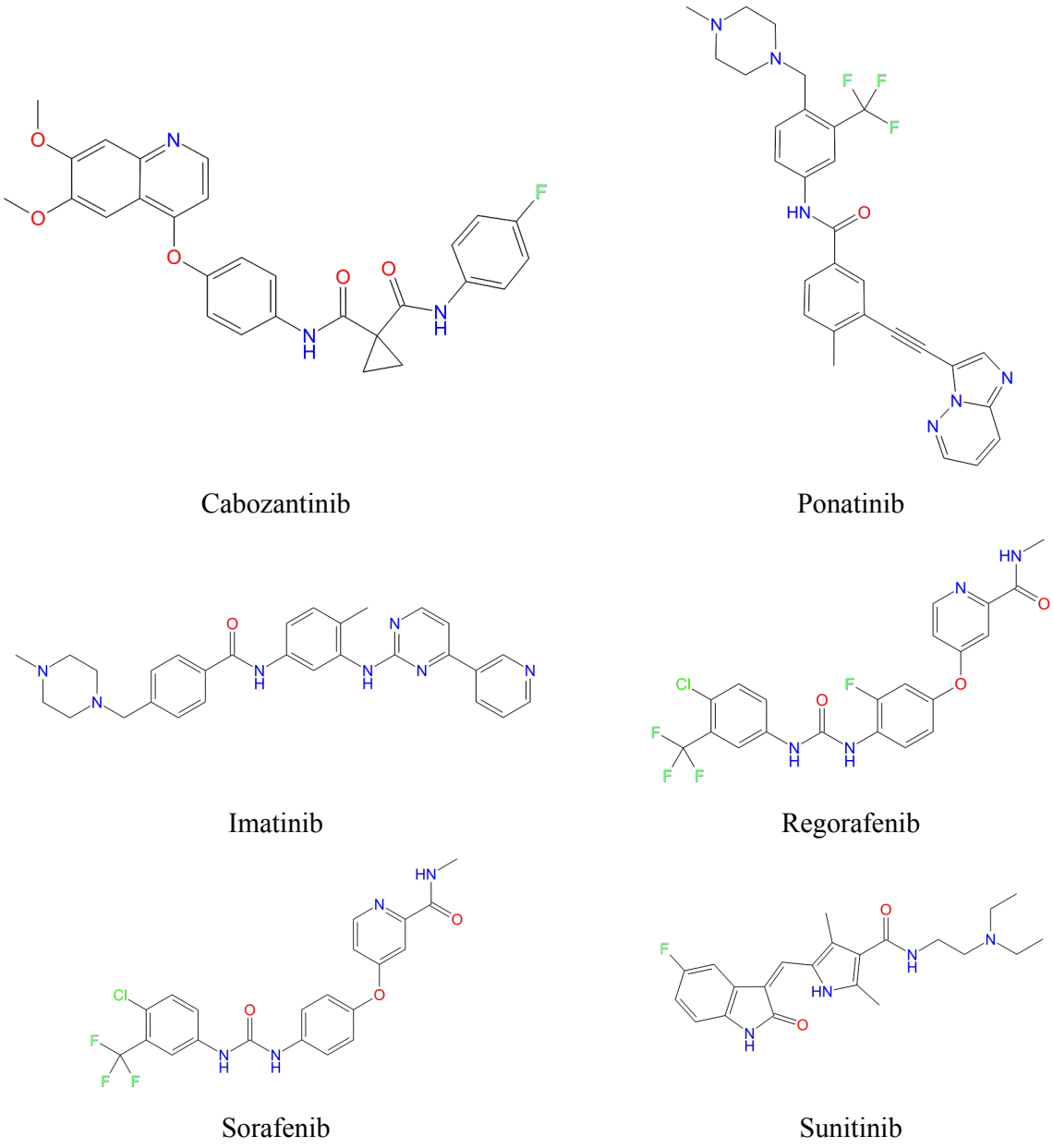

Figure 1. c-Kit known inhibitors.

The first part of this work investigates the most recurrent single-point mutations inserted in the ATP binding pocket like V654A and the mutant T670I, while in the second part, we studied the affinity of the best-ranked molecules in complex with multi-mutated c-Kit proteins, considering also the D816H mutation in the A-loop of the activation region.

The single-point mutated forms (V654A and T670I), complexed with *sunitinib*, and built starting from the selected c-Kit 3D structure (3G0E), have been uploaded to PRIME for energy minimization [20,21], as reported in material and methods.

These new mutated c-Kit forms have been successively processed by Induced Fit Docking (IFD) [22-24], using the well-known drugs reported in Figure 1 as ligands. The overview of the amino acids implicated in the binding at ATP pocket, for all tested drugs, are reported in Table 1, and the amino acids that have the proximity of 2.5 Å to ligands are labeled.

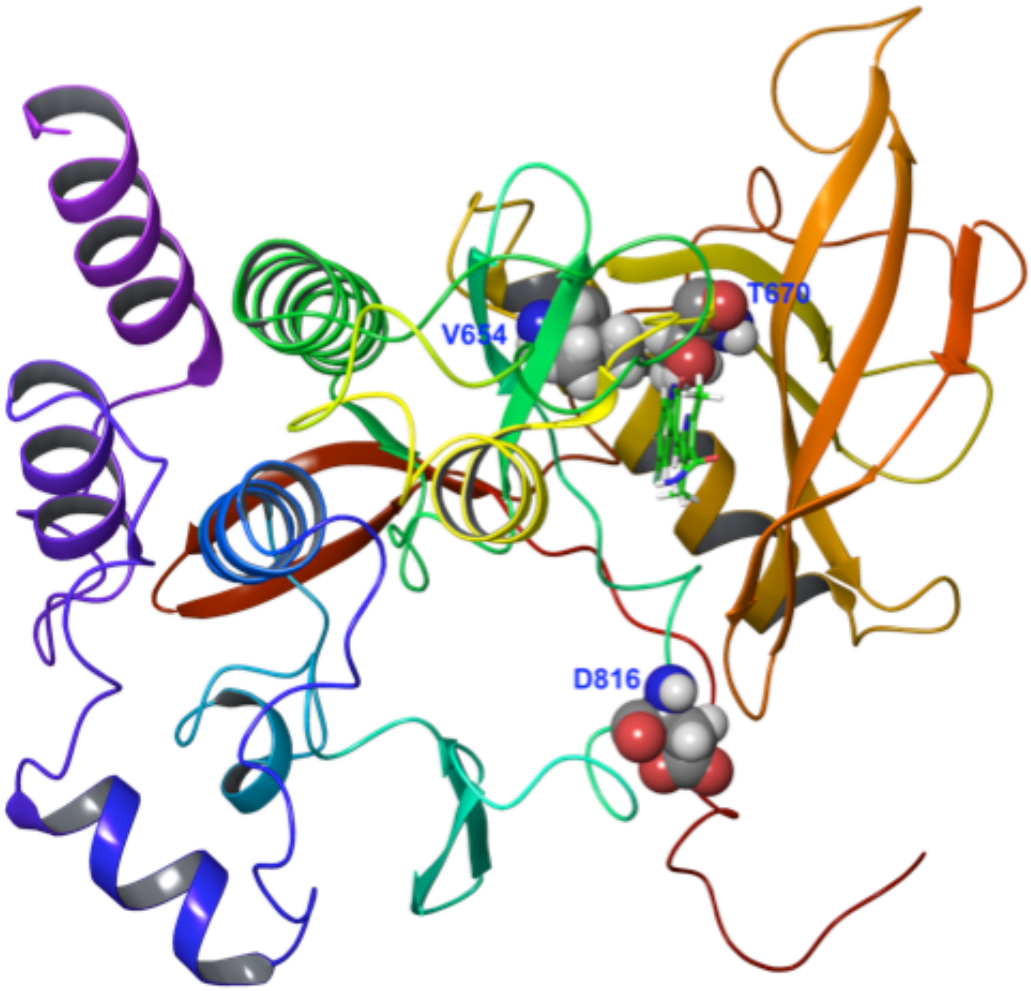

Figure 2. c-Kit kinase domain in complex with *sunitinib* (PDB id: 3G0E): in CPK representation are reported the mutation points V654, T670, and D816; in tube representation is reported the ligand.

All tested drugs (except *sorafenib* in the T670I mutated form) interact with the amino acid F811 of the DFG-motif, strongly connected with the constitutive activation of the c-Kit TKR in cancer cells. The analysis of the data reported in Table 1 confirms the affinity of *imatinib* with c-Kit WT form, involving A621, K623, V654, T670, C673 and F811 amino acids at 2.5 Å proximity, and highlights a reduction in the number of amino acid interactions for the V654A and T670I mutated forms. The more frequent amino acids, which cooperate for the binding mode of the second and third-line inhibitors (*cabozantinib*, *ponatinib*, *sorafenib, sunitinib*, and *regorafenib*), are L595, V603, K623, T670, C673, C674, M757, F811, A814 (Table 1). All these residues are not strictly involved in the interactions between *imatinib* and the three TKR forms under investigation, suggesting their role in increasing the affinity binding of the new generations inhibitors with the TKR mutated forms. The analysis of the 2D amino acids (AA) maps (see SI), points out the recurrent formation of donor and acceptor hydrogen bonds between the crucial amino acid C674 and the NH functional groups reported in *sunitinib, regorafenib*, and *sorafenib*. Furthermore,

ionic interactions and hydrogen bonds are formed between the AA residues E671, E758 and the nitrogen atoms of *cabozantinib*, *sunitinib*, and *regorafenib*.

Table 1. Overview of the amino acids involved in the binding of the selected known drugs in the ATP binding site at 2.5 Å proximity.

		Amino Acid																							
Drug	c-Kit form	**K593**	**L595**	**V603**	**A621**	**K623**	**V654**	**T670**	**E671**	**Y672**	**C673**	**C674**	**G676**	**D677**	**N680**	**R684**	**M757**	**E758**	**C809**	**F811**	**A814**	**D820**	Number of AA at 2.5 Å
Imatinib	WT	X			X	X	X	X			X									X			7
	V654A	X				X		X				X								X			5
	T670I	X					X	X			X									X			5
Cabozantinib	WT		X	X		X		X	X	X	X			X			X	X		X	X		12
	V654A		X	X		X		X	X	X	X			X			X	X		X	X		12
	T670I		X	X		X		X	X	X	X			X			X	X	X	X	X		13
Ponatinib	WT		X				X						X	X						X	X	X	X	8
	V654A		X								X		X	X						X	X	X		7
	T670I		X					X			X		X	X		X				X	X	X	X	10
Sorafenib	WT		X	X		X	X	X		X	X	X					X	X		X			11
	V654A		X	X		X		X			X	X					X	X		X			9
	T670I		X			X		X		X	X	X						X					7
Sunitinib	WT					X	X	X	X		X	X					X	X		X			9
	V654A					X		X	X		X	X					X	X		X			8
	T670I					X	X	X	X		X	X					X	X		X			9
Regorafenib	WT	X	X	X		X					X	X			X		X	X		X			10
	V654A	X	X	X								X			X		X	X		X			8
	T670I	X	X	X		X		X				X			X		X	X		X			10

The docking XP results (Table 2) confirm the trend of the binding affinity between selected inhibitors and the three c-Kit proteins (WT, V654A, and T670I), in agreement with the experimental data obtained in the clinical treatments [25]. *Imatinib*, an inhibitor of first-line treatment, shows the highest affinity binding for the WT protein while no well-fitting with the other c-Kit mutated forms (V654A and T670I), is observed.

To validate molecular docking studies, Spearman's rank correlation coefficient ϱ has been applied. This statistic approach is a rank-based measure of association between the wet-lab bioassay values and the reported docking scores. The inhibitors under investigation are *imatinib*, *sorafenib*, and *sunitinib* for which the Kds are available. The ϱ value of 0.93 state the validation of the molecular docking protocol (Supplementary material, S1).

Further analysis of the molecular docking results shows as *sunitinib* and the other inhibitors of the second and third-line treatments [26-28], maintaining the affinity for the c-kit WT form, exhibit better binding scores with the two mutated kinases.

Table2. IFD scores of the selected known c-Kit inhbitors.

Drug	**WT**	**V654A**	**T670I**
	Docking scores		
Imatinib	-10.187	- 9.010	- 6.110
Cabozantinib	-10.712	-11.655	-12.168
Ponatinib	- 9.811	-11.401	-10.854
Sorafenib	- 9.687	-11.861	- 9.853
Sunitinib	- 9.744	-10.782	-10.355
Regorafenib	-11.139	-12.664	-12.426

In Figure 3, the binding poses of *imatinib (*first line-treatment*)* are compared with that of *cabozantinib* (second line-treatment) into the ATP-binding region of the WT (a), and V654A (b) T670I (c) mutated isoforms, in order to emphasize the amino acids involved in the complexes. Full data of the amino acids representations are reported as supplementary material (S2).

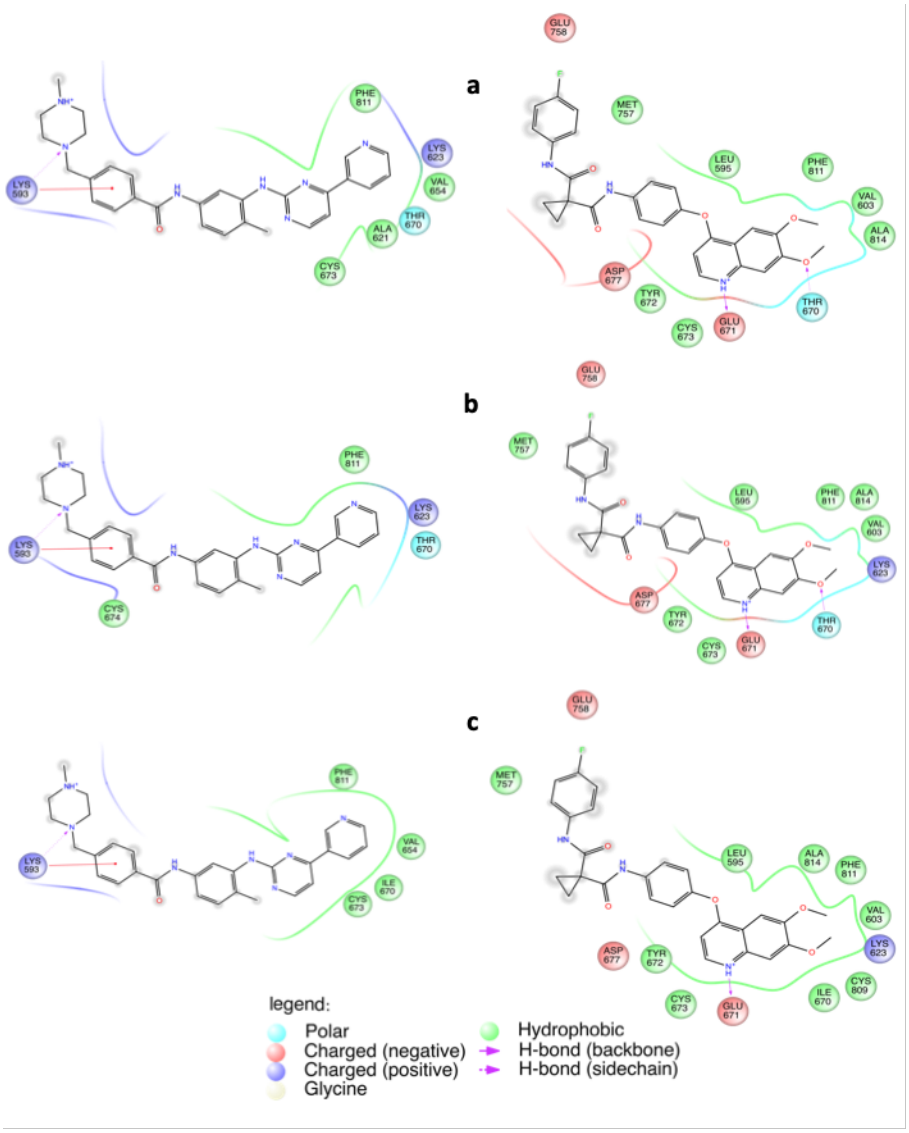

Figure 3. Representation of ligands interactions at ATP binding site: *imatinib* vs *cabozantinib* (**a**, WT c-kit protein; **b**, V654A single-point mutated form; **c**, T670I single-point mutated form).

The number of amino acids at 2.5 Å of proximity, closely interacting with the drugs of new generation (i.e. *cabozantinib*, Figure 2 - right), is higher than that observed for the TKR protein complexes with *imatinib* (Figure 2 – left). This outlines, that the shape of the inhibitors, able to overcome tumor resistance, is better suited in the ATP regions of both WT and mutated forms. With this regard, the binding poses of *imatinib,* and *cabozantinib,* at the ATP binding site of the T670I mutated form (Figure 4), show how *cabozantinib* is buried in the ATP cavity deeper than *imatinib*, and point out the pivotal importance of the interaction between the amino acid I670 and the dimethoxy substituents on the phenyl moiety.

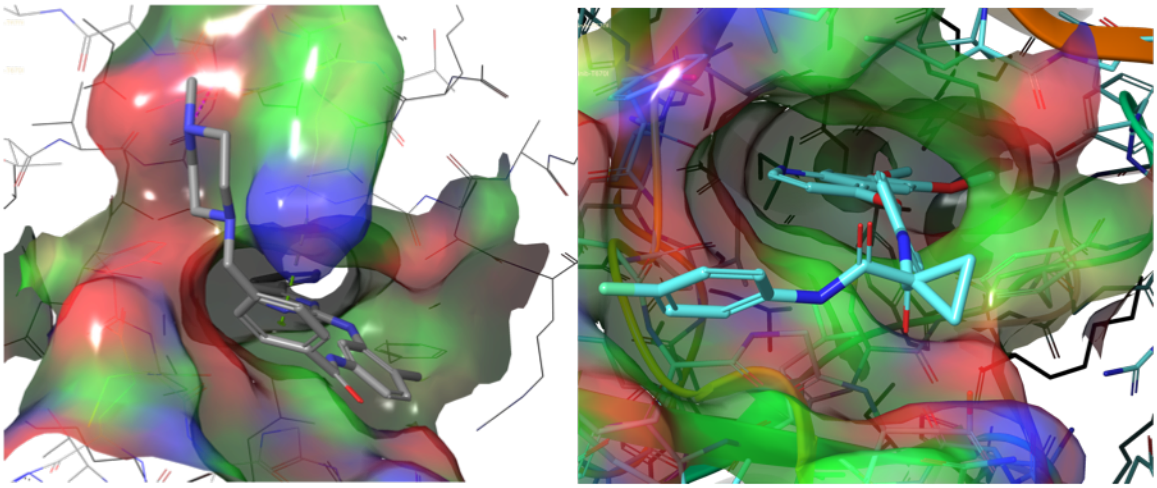

Figure 4. Docking poses of *imatinib* (left) and *cabozantinib* (right), in the ATP binding pocket of the T670I mutated form.

2.2. Identification of new c-Kit ATP binding site ligands

A set of new molecules is identified as possible selective c-Kit modulators starting from the 3D c-Kit structures (WT and the rebuilt mutated isoforms) and the amino acids site map information, obtained by the above *in silico* studies.

In particular, a database of thousands of commercial compounds was submitted to a sequence of ligand and structure-based methods, flowing the procedure schematically described in Figure 5.

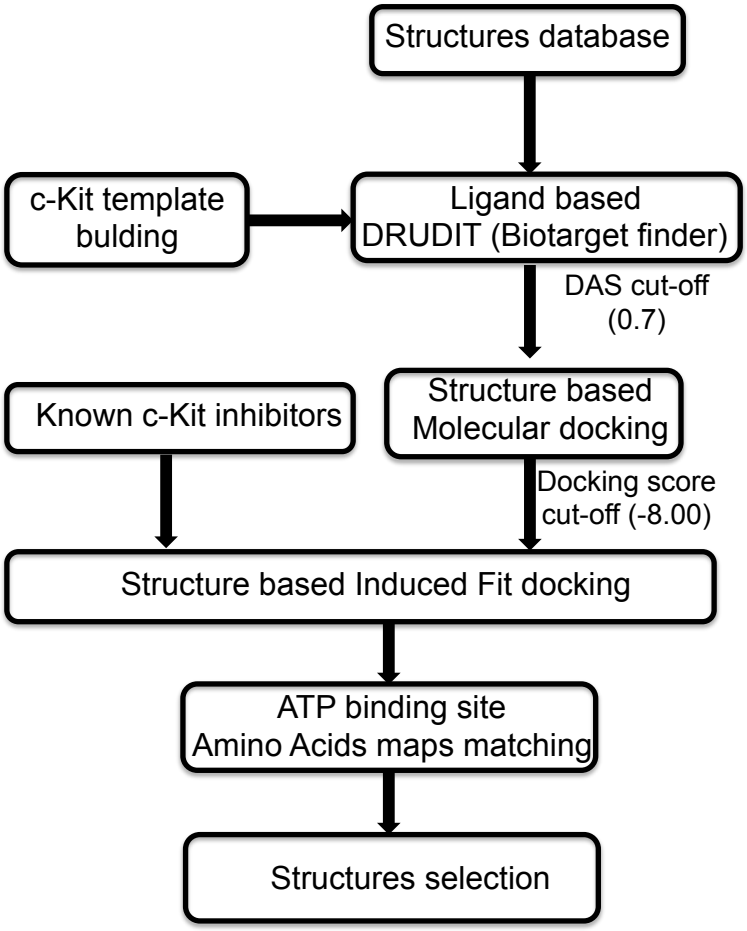

Figure 5. Flow-chart of the applied protocol.

2.2.1. Ligand based DRUDIT Biotarget Finder

The first analyzed protocol is the application of the Biotarget Finder tool available on the web-server DRUDIT (www.drudit.com) [29,30], adopting a ligand-based approach based on the selection of several molecular descriptors. The robustness of this method in the discovery of new antitumor lead compounds has been previously demonstrated [31-38]. The crucial step of the protocol is the matching of the molecules database with the template of the receptor under investigation, built through calculated molecular descriptors. The template of c-Kit receptor has been built, selecting a set of well-known c-Kit modulators endowed with IC_{50} values at sub-micromolar concentration [24]. Then the external target has been uploaded in DRUDIT web-server [29,30], and the whole database of structures has been submitted to the Biotarget Finder tool with default parameters. From the output matrix of this *in silico* ligand-based protocol, a set of molecules with a Drudit Affinity Score (DAS) upper to 0.7 is selected and used for the subsequent molecular docking structure-based analysis (supplementary material S3).

2.2.2. Structure based Molecular docking

The molecular docking settings, above mentioned for the validation of native ligands (materials and methods section), has been adopted for the docking analysis of the molecules selected by the ligand-based protocol (721 hits) into the ATP binding cavity of c-Kit WT protein. A total number of 36 best–fitting molecules have been identified fixing a

cut-off of docking score at -8.00. A further selection was performed by considering a series of filters well consolidated in the search of bioactive compounds, such as 1) PAINS filters [39]; 2) Lipinski's rule [40]; 3) Veber rules [41]; 4) Egan rules [42]. Thus, the 36 molecules previously selected have been submitted to SwissADME web-facilities as available at http://www.swissadme.ch [43]. The molecules resulting at the end of the screening procedure are reported in bold in Table 3.

Table 3. Selection of the hits by conventional filters to screen bio-active compounds.

Molecule ID	MW	#H- acceptors	#H- donors	MR	iLOGP	Lipinski #violations	Veber #violations	Egan #violations	PAINS #alerts
39753	400.47	4	0	116.63	0.26	0	0	0	0
45350	261.12	2	1	59.67	2.24	0	0	0	0
55607	418.47	3	3	123.19	2.04	0	0	0	0
55723	426.51	4	0	124.29	0.28	1	0	0	0
56561	430.50	5	0	122.96	0.53	0	0	0	0
71106	506.64	6	4	136.91	2.89	1	2	1	0
76308	522.64	5	4	147.43	2.63	1	2	1	0
78510	245.25	3	2	65.32	1.07	0	0	0	0
223948	452.42	9	3	114.51	1.32	1	1	1	0
271462	441.40	8	5	117.44	0.15	1	1	1	0
534218	238.06	2	1	54.69	1.84	0	0	0	0
630705	222.24	3	1	57.93	1.11	0	0	0	0
630713	206.17	4	1	52.70	1.02	0	0	0	0
748439	199.25	1	2	61.46	1.79	0	0	0	0
754137	210.27	0	2	73.3	2.03	0	0	0	1
A202	386.41	7	5	101.27	1.42	0	1	1	1
A5877	235.22	4	2	61.43	0.85	0	0	0	2
C7493	393.44	6	2	108.69	2.95	0	0	0	0
D7006	441.40	8	5	117.44	0.15	1	1	1	0
D7635	393.50	3	2	115.20	2.41	0	0	0	0
L2411	452.54	4	1	135.78	3.56	0	0	0	0
M1000000	452.42	9	3	114.51	1.32	1	1	1	0
M7824	452.42	9	3	114.51	1.32	1	1	1	0
O3264	370.45	5	4	106.90	2.93	0	0	0	1
P8477	376.41	5	2	103.49	2.15	0	0	0	0
PZ0293	391.37	6	0	105.39	3.06	0	0	0	0
S4568	345.36	5	1	96.74	2.70	0	0	0	0
S9692	371.45	4	2	104.72	2.75	0	0	0	0
SML0140	376.34	5	0	101.79	1.96	0	0	0	0

SML0314	445.56	3	4	136.72	4.06	0	0	0	0
SML0574	342.46	2	1	99.76	2.99	0	0	0	0
SML1084	447.50	4	1	132.71	3.36	1	0	0	0
SML1307	352.38	5	2	101.01	2.71	0	0	0	0
SML1348	461.53	6	1	124.73	3.09	0	0	0	0
SML1352	457.59	2	5	140.22	3.81	0	0	0	0
SML1660	446.52	4	2	132.48	4.24	0	0	0	0

The 24 top-scored molecules (depicted in Figure 6) have been examined by Induced-Fit studies to evaluate the binding affinity (Table 4) and analyse the amino acids involved in the three different ATP binding pockets (WT, V654A and T670I mutated proteins).

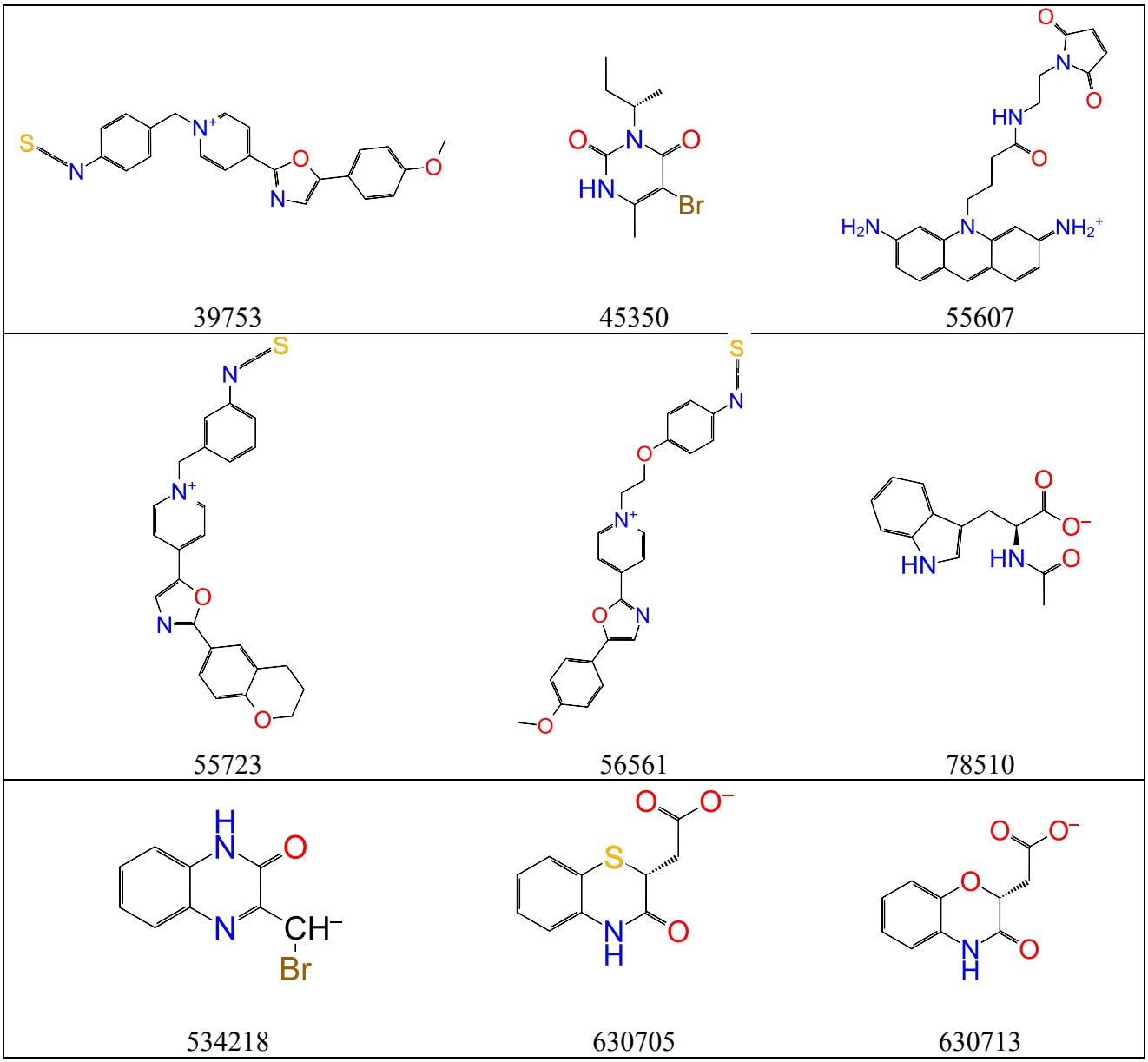

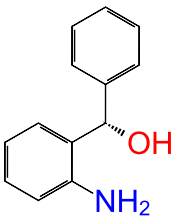

748439

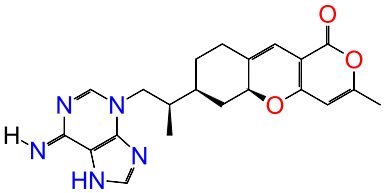

C793

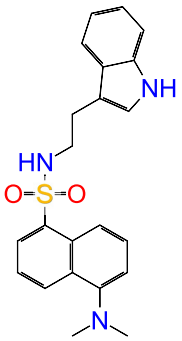

D7635

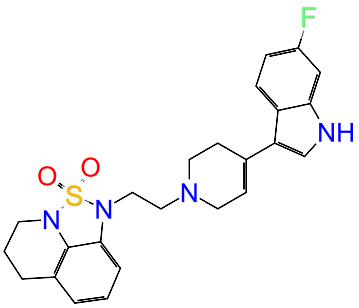

L2411

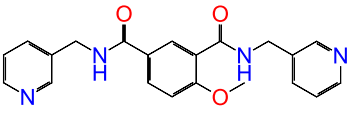

P8477

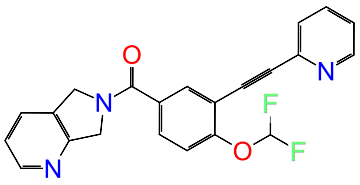

PZ0293

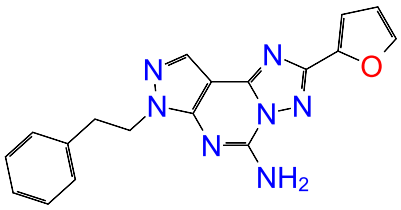

S4568

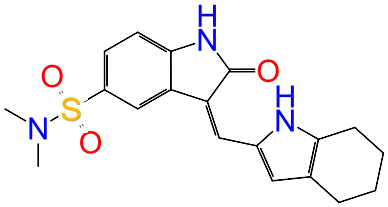

S9692

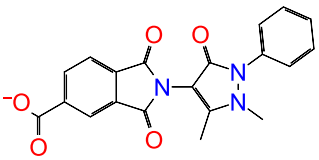

SML0140

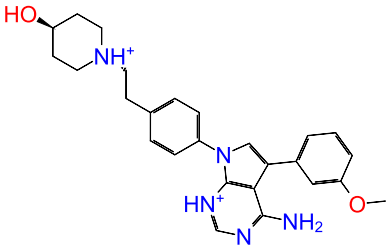

SML0314

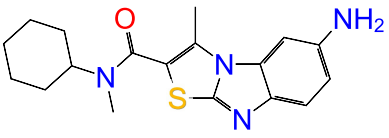

SML0574

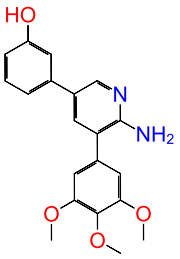

SML1307

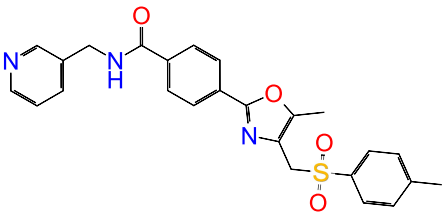

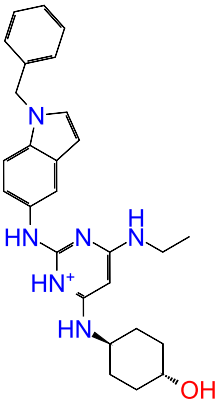

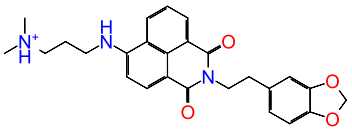

SML1348	SML1352	SML1660

Figure 6. Top scored hits identified.

The results have been finally compared with those previously obtained for the known TKR inhibitors of the first and second-line treatments (Supplementary material, S4). In general, the set of amino acids involved in the binding are similar to that highlighted for the interactions with *cabozantinib*, *regorafenib*, and *ponatinib* (see above, 2.1. paragraph).

The data processing has been aimed at evaluating the docking score differences between the c-Kit WT protein and the mutated forms. In particular, the molecules with a ΔGscore between the mutated forms and the WT form higher than 1 have been selected (Table 4).

Table 4. IFD Molecular docking results (XP scores) of the top scored molecules.

*ID	WT-**X**P GScore	V654A-**X**P GScore	T670I-**X**P GScore	**ΔGScore V-WT**	**ΔGScore T-WT**
39753	-9.986	-9.689	-9.508	0.297	0.478
45350	-8.690	-8.885	-8.917	-0.195	-0.227
55607	-10.428	-10.803	-11.022	-0.375	-0.594
55723	-9.184	-7.99	-9.219	1.194	-0.035
56561	-9.702	-9.668	-9.552	0.034	0.150
78510	-9.056	-7.775	-10.162	1.281	-1.106
534218	-8.030	-8.483	-9.415	-0.453	-1.385
630705	-8.532	-8.411	-9.861	0.121	-1.329
630713	-9.617	-9.126	-9.807	0.491	-0.190
748439	-9.939	-9.249	-9.375	0.690	0.564
C7493	-9.756	-8.326	-8.802	1.430	0.954
D7635	-10.055	-9.163	-10.134	0.892	-0.079
L2411	-9.644	-9.315	-9.802	0.329	-0.158
P8477	-9.462	-9.060	-9.383	0.402	0.079
PZ0293	-7.945	-8.846	-9.440	-0.901	-1.495
S4568	-10.443	-8.420	-7.817	2.023	2.626
S9692	-9.765	-10.024	-10.065	-0.259	-0.300
SML0140	-8.918	-10.290	-9.790	-1.372	-0.872
SML0314	-11.015	-10.86	-11.193	0.155	-0.178
SML0574	-8.980	-9.167	-8.267	-0.187	0.713
SML1307	-12.488	-11.346	-13.300	1.142	-0.812
SML1348	-6.856	-10.517	-7.955	-3.661	-1.099
SML1352	-9.702	-8.840	-9.684	0.862	0.018
SML1660	-12.859	-10.041	-11.830	2.818	1.029

*in bold were highlighted the selected structures.

Thus, the analysis of the data reported in Table 4, shows how the derivatives 78510, 534218, 630705, and PZ0293 are the best candidates to interact with T670I c-Kit mutated

form, while molecules SML0140, SML1348 appear more inclined to complex V654A mutated protein.

The overview of the amino acids involved in the ligand-protein binding at 2.5 Å of proximity is reported in Table 5. The six selected molecules interact with the amino acids L595, V603, K623, V654A, T670I, C673, and F811, consistently with the pivotal amino acid residues highlighted in the analysis of the binding mode of c-kit second and third-line inhibitors.

Table 5. Overview of amino acids, interacting with the selected structures in the binding with the ATP regions of c-Kit forms.

c-Kit forms	ID	LYS 593	LEU 595	GLY 596	VAL 603	ALA 621	LYS 623	VAL 654	THR 670	GLU 671	TYR 672	CYS 673	CYS 674	GLY 676	ASP 677	ASN 680	ARG 684	MET 757	GLU 758	LEU 799	CYS 809	ASP 810	PHE 811	GLY 812	LEU 813	ALA 814	#AA
WT			✔		✔	✔	✔	✔	✔	✔	✔	✔	✔	✔						✔							12
V654A	78510		✔		✔	✔	✔		✔	✔		✔								✔			✔				9
T670I			✔		✔		✔	✔	✔	✔	✔	✔		✔						✔			✔			✔	12
WT			✔		✔	✔					✔	✔		✔									✔				7
V654A	534218		✔		✔		✔	✔	✔	✔	✔	✔											✔				9
T670I			✔		✔	✔	✔	✔	✔		✔	✔										✔	✔			✔	11
WT			✔		✔	✔	✔	✔	✔	✔	✔	✔								✔		✔	✔			✔	13
V654A	630705		✔		✔		✔		✔	✔	✔	✔		✔						✔			✔			✔	11
T670I		✔	✔		✔	✔	✔	✔	✔	✔	✔	✔		✔						✔			✔			✔	14
WT			✔		✔	✔	✔	✔	✔	✔	✔	✔	✔		✔				✔	✔		✔	✔				15
V654A	PZ0293	✔	✔		✔	✔	✔	✔	✔	✔	✔	✔		✔					✔	✔	✔	✔	✔				16
T670I		✔	✔		✔	✔				✔	✔	✔	✔						✔				✔				10
WT			✔		✔	✔	✔	✔		✔	✔	✔	✔	✔									✔				11
V654A	SML0140	✔	✔		✔	✔	✔	✔	✔	✔	✔	✔								✔			✔	✔	✔	✔	15
T670I		✔			✔	✔	✔	✔	✔	✔	✔	✔								✔		✔	✔		✔	✔	14
WT		✔		✔	✔	✔	✔	✔		✔	✔	✔	✔	✔	✔		✔		✔	✔			✔			✔	16
V654A	SML1348		✔	✔	✔	✔	✔	✔	✔	✔	✔	✔	✔			✔		✔	✔	✔	✔		✔			✔	18
T670I		✔	✔		✔	✔	✔	✔	✔		✔	✔	✔	✔	✔	✔	✔			✔	✔		✔			✔	18

The selected ligands show a suitable fit with the T670I mutated kinase form, establishing close interactions with the mutated amino acid I670 in the ATP-binding site, and the best-scored ligand 3,4-dihydro-3-oxo-2H-(1,4)-benzothiazin-2-ylacetic acid (630705) is reported in Figure 7 (left). Furthermore, also SML0140 and SML1348 were found to be valuable modulators of V654A mutated form, due to the electrostatic bonds with A654. The best ranked ligand (SML1348) is reported in Figure 7 (right).

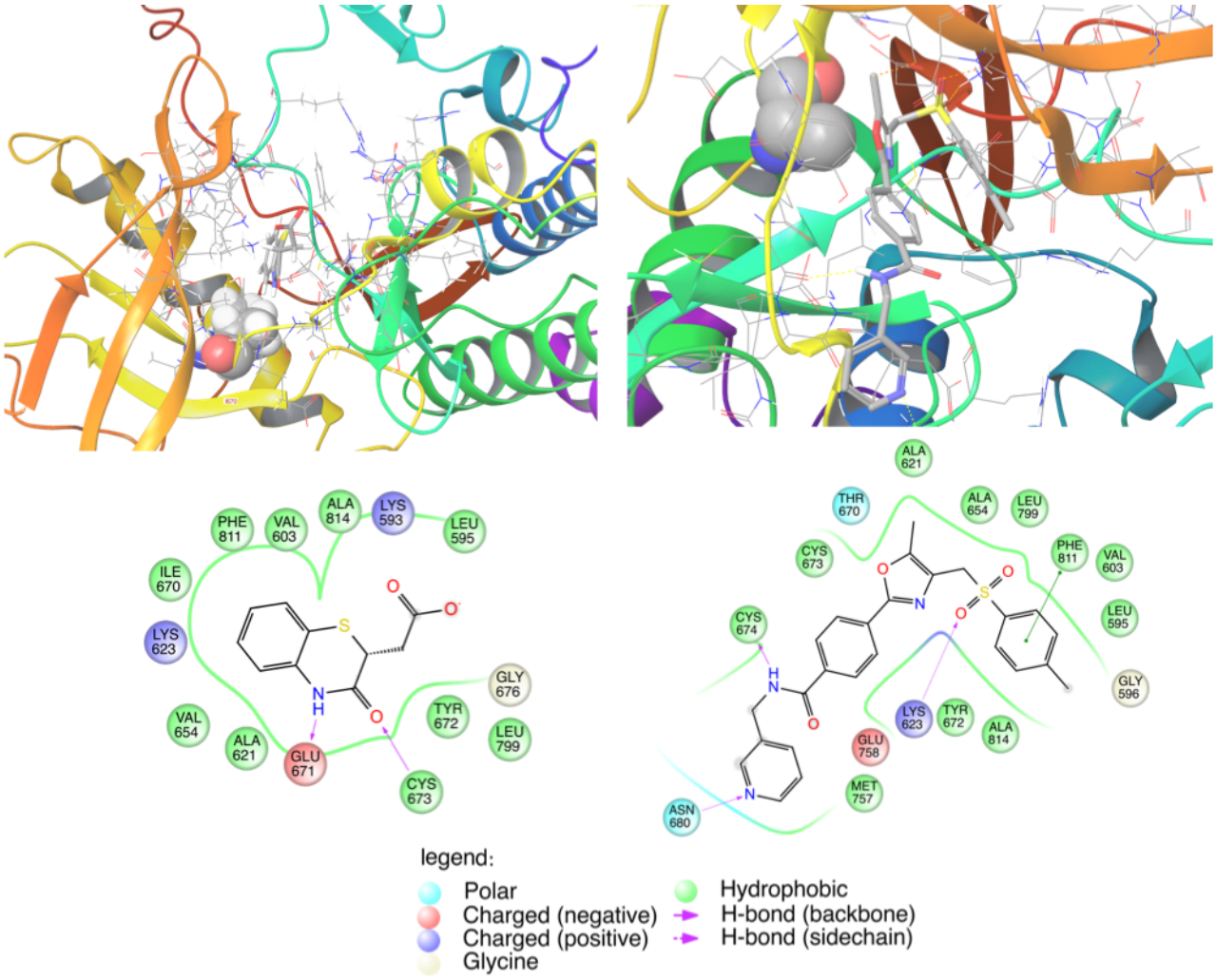

Figure 7. Binding sites representation of the 3D binding modes (upper) and maps (down) of the 630705 (left, T670I c-kit mutated form), and SML1348 (right, V654A c-kit mutated form).

The analysis of the binding mode of the selected molecules confirms a promising binding capability at the ATP binding pocket. In fact, as observed in the case of *cabozantinib* (Figure 3), the ligands are buried in the cavity close to I670 (Figure 7, left upper) and the A654 (Figure 7, right upper). In particular, analyzing the 2D AA map (Figure 7, left lower), the NH and carbonyl moieties of the molecule 630705 establish donor and acceptor hydrogen bonds with the amino acids E671, C673. Compound SML1348 (Figure 7, right, lower), interacts with the ATP active region, bonding the amino acid residues N680, C673, and K623 with donor and acceptor hydrogen interactions. The aryl moiety of the ligand forms cation-π interaction with the pivotal amino acid F811.

2.3. Comparative XP docking

In order to evaluate the behavior of the selected derivatives in presence of two (I670 and A654) and three (I670, A654, and H816) simultaneously mutations, IFD docking studies have been carried out. In particular, the respective proteins have been built and optimized following the same protocol used previously for the c-Kit single-point mutated forms. Table 7 shows the IFD docking results. The selected hits are compared with *imatinib*

and *sunitinib*, and, as expected, the docking score data confirm the weak capability of *imatinib* to complex the mutated forms both with two I670-A654 (IA) and three mutations I670-A654-H816 (IAH), providing the worst results. Docking scores assign to *sunitinib*, for both the mutated cases (IA and IAH), a high rank, demonstrating its efficaciousness as c-Kit modulator. Finally, the data acquired for the SML0140 and 78510 (Table 7) suggest a promising capability of these molecules to overcome D816H acquired resistance, showing values comparable to that of *sunitinib.*

Table 7. Molecular XP docking results of the studied molecules into mutated proteins (IA, IAH).

Derivative	IA	IAH
	Docking score	
Imatinib	-8.58	-7.37
Sunitinib	-10.88	-9.67
78510	-8.322	-9.404
534218	-5.078	-8.851
630705	-6.631	-8.555
PZ0293	-6.328	-7.673
SML0140	-8.728	-9.702
SML1348	-6.491	-8.157

3. Conclusions

The mixed ligand- and structure-based *in silico* protocols applied in this study allow us to identify a set of molecules as new potential modulators of c-Kit mutated proteins able to overcome the most frequent acquired resistance in the clinical treatment of cancer.

One of the advantages of the method is the possibility to easily explore previously developed ligand-based protocols, available through the web-server DRUDIT; this last, in fact, provides a rapid and non-conventional selection of new potential modulators of c-Kit. The ligand-based methods, based on the molecular descriptors, allow for selecting heterogeneous structures, not constrained by steric reasons to the binding cavity. The further structure-based study can be performed rapidly and leads to identify the best features, required to the c-Kit modulators to overcome the tumour cell resistance.

The protocol, therefore, permits identifying a set of structures with a significant binding capability, almost comparable to known drugs, and with a potential selectivity against the mutated forms. In particular, the derivatives 78510, 534218, 630705, and PZ0293 are identified as successful candidates to interact with T670I c-Kit mutated form, while molecules SML0140, SML1348 appear more incline to complex V654A mutated protein.

In general, the six selected molecules interact with the amino acids L595, V603, K623, V654A, T670I, C673, and F811, in agreement with the pivotal amino acid residues highlighted in the analysis of the binding mode of c-Kit inhibitors of second and third-line treatments. Finally, exploring the interactions with the multi-mutated forms I670-A654

(IA), and three, I670-A654-H816 (IAH), SML0140 shows a significant binding score against the mutated form IAH if compared with the known drugs.

4. Materials and Methods

4.1. Structure based studies

The ligands and protein–ligand complex used for the in silico studies were prepared as follows:

4.1.1. Ligand Preparation

The default setting of the LigPrep tool implemented in Schrödinger's software has been used to prepare the ligands for docking [44]. All possible tautomers and a combination of stereoisomers have been generated for pH of 7.0 ± 0.4, using the Epik ionization method [45]. Energy minimization is subsequently done using the integrated OPLS 2005 force field [46].

4.1.2. Proteins Preparation

The high-resolution crystal structure of c-Kit (PDB ID: 3G0E) [12] is downloaded from the Protein Databank [47]. All water molecules were deleted using Protein Preparation Wizard of Schrödinger software that is subsequently employed for further preparations of the protein structure using the default settings [48].

Bond orders have been assigned and hydrogen atoms added as well as protonation of the heteroatom states using Epik-tool (with the pH set at biologically relevant values, i.e. at 7.0 ± 2.0). The H-bond network has been then optimized. The structure is finally subjected to a restrained energy minimization step (rmsd of the atom displacement for terminating the minimization was 0.3 Å), using the Optimized Potentials for Liquid Simulations (OPLS) 2005 force field [46].

The optimized c-Kit crystal structure is also used as a starting point to build the mutated forms (V654A, T670I, IA, and IAH). In details, point mutations are applied by sequence viewer tools, available in MAESTRO suite. The resulting structures are optimized by PRIME module.

Finally, as the results from each refinement run are examined, the quality of each model has been further validated through the Ramachandran Plot generated, which shows a low fraction of all residues (< 2.8-4.0 %) falling outside the favourable regions.

4.1.3. Docking Validation

Molecular Docking is performed by Glide program [49-51]. The receptor grid preparation has been carried out by assigning the original ligand (*sunitinib*) as the centroid of the grid box. The generated 3D conformers are docked into the receptor model using the Standard Precision (SP) mode as the scoring function. A total of 5 poses per ligand conformer are included in the post-docking minimization step, and a maximum of 2 docking poses are generated for each ligand conformer. The proposed docking procedure

is validated by the re-dock of the crystallized *sunitinib* within the receptor-binding pockets of 3G0E (WT form) and 3G0F (mutated D816H form). The results obtained are in significant agreement with the experimental poses, showing a rmsd of 0.75 and 0.92 for the 3G0E and 3G0F, respectively. Moreover, to validate the docking scores the comparison of GLIDE score-in-place and flexible functions (XP mode) was performed on 3G0E obtaining comparable values (-9.59 and -9.75 respectively).

4.1.4. Induced Fit Docking

Induced fit docking simulation is performed using the IFD application as available [52,53] in the Schrödinger software suite [54], which is demonstrated to be an accurate and robust method to account for both ligand and receptor flexibility [55]. The atomic coordinates for c-Kit are downloaded from the Protein Data Bank (PDB id 3G0E) and submitted to the Protein Preparation Wizard module in Schrödinger as follows: adding hydrogen, assigning partial charges (using the OPLS-2001 force field) and protonation states. All crystal waters have been removed.

The IFD protocol is carried out as follows [56, 57]: the ligands are docked into the rigid receptor models with scaled-down van der Waals (vdW) radii. The Glide Standard Precision (SP) mode [49-51] is used for the docking, and 20 ligand poses are retained for protein structural refinements. The docking boxes are defined to include all amino acid residues within the dimensions of 25 Å × 25 Å × 25 Å from the center of the original ligands; the induced-fit protein–ligand complexes are generated using the Prime software [58, 59]. The structures obtained from the previous step are submitted to side-chain and backbone refinements. All residues with at least one atom located within 5.0 Å of each corresponding ligand pose are included in the refinement by Prime. All the poses generated are then hierarchically classified, refined and further minimized into the active site grid before being finally scored using the proprietary GlideScore function, defined as: GScore= 0.065*vdW + 030*Coul + Lipo + Hbond + Metal + BuryP + RotB + Site, where: vdW is the van der Waals energy term, Coul is the Coulomb energy, Lipo is a Lipophilic contact term which rewards favorable hydrophobic interactions, Hbond is an H-bonding term, Metal is a metal-binding term (where applicable), BuryP is a penalty term applied to buried polar groups, RotB is a penalty for freezing rotatable bonds and Site is a term used to describe favourable polar interactions in the active site.

Finally, IFD score (IFD score = 1.0 Glide_Gscore + 0.05 Prime_Energy), which accounts for both protein–ligand interaction energy and total energy of the system, is calculated and used to rank the IFD poses. The more negative is the IFDscore, the more favorable is the binding.

4.2. Biotarget Finder module (DRUDIT)

The selection of suitable c-Kit inhibitors is performed through the module Biotarget Finder as available in the web-server www.drudit.com [30]. The tool allows predicting the binding affinity of candidate molecules versus the selected biological target. The template of the biological target is built by using a set of known modulators. The selected

structures, well-known inhibitors of c-Kit, are acquired from the binding database [35] and are further filtered by applying a cut-off of 1 μM to IC50. The resulting structures are uploaded to web-server as external targets, to get the c-Kit template. The entire database is submitted to the Biological Predictor module by using the default parameters, and the output results are obtained as DAS (Drudit Affinity Score) for each structure.

Supplementary Materials: The following are available online: S1, Spearman's rank correlation test; S2, amino acids maps of known drugs; S3, S2-DRUDIT results, S4, amino acids maps of the selected compounds.

Author Contributions: Both authors have contributed equally to this work.

Funding: This research received no external funding.

Conflicts of Interest: The authors declare no conflict of interest.

References

1. Cooper GM. The Cell: A Molecular Approach. 2nd edition. Sunderland (MA): Sinauer Associates; **2000**.
2. Fouad YA, Aanei C. Revisiting the hallmarks of cancer. *Am J Cancer Res*. **2017**, 7(5), 1016–1036.
3. Hassan M, Watari H, AbuAlmaaty A, Ohba Y, Sakuragi N. Apoptosis and molecular targeting therapy in cancer. *Biomed Res Int*., **2014**, 150845.
4. Srivastava S, Grizzle WE. Biomarkers and the genetics of early neoplastic lesions. *Cancer Biomark*. **2010**, 9(1-6), 41–64.
5. Gentile, C.; Martorana, A.; Lauria, A.; Bonsignore, R. Kinase Inhibitors in Multitargeted Cancer Therapy. *Curr. Med. Chem.*, **2017**, *24(16)*, 1671-1686.
6. Sweeny, L.; Zimmermann, T.M.; Liu, Z.; Rosenthal, E.L. Evaluation of Tyrosine Receptor Kinases in the Interactions of Head and Neck Squamous Cell Carcinoma Cells and Fibroblasts. *Oral Oncol.*, **2012**, *48*, 1242-1249.
7. Yamauchi, T.; Yamauchi, N.; Ueki, K.; Sugiyama, T.; Waki, H.; Miki, H.; Tobe, K.; Matsuda, S.; Tsushima, T.; Yamamoto, T.; Fujita, T.; Taketani, Y.; Fukayama, M.; Kimura, S.; Yazaki, Y.; Nagai, R.; Kadowaki, T. Constitutive Tyrosine Phosphorylation of ErbB-2 *via* Jak2 by Autocrine Secretion of Prolactin in Human Breast Cancer. *J. Biol. Chem.*, **2000**, *275*, 33937-33944.
8. Tsai, C.J.; Nussinov, R. The Molecular Basis of Targeting Protein Kinases in Cancer Therapeutics. *Semin. Cancer Biol.*, **2013**, *23*, 235-24.
9. Bodemer, C.; Hermine, O.; Palmerini, F.; Yang, Y.; Grandpeix-Guyodo, C., Leventhal, P.S.; Hadj-Rabia, S.; Nasca, L.; Georgin-Lavialle, S.; Cohen-Akenine, A.; Launay, J.M.; Barete, S.; Feger, F.; Arock, M.; Catteau, B.; Sans, B.; Stalder, J.F.; Skowron, F.; Thomas, L.; Lorette, G.; Plantin, P.; Bordigoni, P.; Lortholary, O.; de Prost, Y.; Moussy, A., Sobol, H.; Dubreuil, P. Pediatric mastocytosis is a clonal disease associated with D816V and other activating c-KIT mutations. *J. Invest. Dermatol.,* 2010, *130 (3)*, 804-015.
10. Ashman, L.K. The biology of stem cell factor and its receptor C-kit. *Int. J. Biochem. Cell Biol.*, **1999**, *31(10)*,1037-51.
11. Duensing, A.; Heinrich, M.C.; Fletcher, C.D.; Fletcher, J.A. Biology of gastrointestinal stromal tumors: KIT mutations and beyond. *Cancer Invest.*, **2004**, *22(1)*,106-16.

12. Mol, C.D.; Dougan, D.R.; Schneider, T.R.; Skene, R.J.; Kraus, M.L.; Scheibe, D.N.; Snell, G.P.; Zou, H.; Sang, B.C.; Wilson, K.P. Structural basis for the autoinhibition and STI-571 inhibition of c-Kit tyrosine kinase *J. Biol. Chem.*, **2004**, *279(30)*, 31655-31663.
13. Chauvot de Beauchêne, I.; Allain, A.; Panel, N.; Laine, E.; Trouvé, A.; Dubreuil, P.; L. Hotspot Mutations in KIT Receptor Differentially Modulate Its Allosterically Coupled Conformational Dynamics: Impact on Activation and Drug Sensitivity. *PLoS Comput. Biol.* **2014**, *10(7),* e1003749, 1-25.
14. Tamborini, E.; Bonadiman, L.; Greco, A.; Albertini, V.; Negri, T.; Gronchi, A.; Bertulli, R.; Colecchia, M.; Casali, P.G.; Pierotti, M.A.; Pilotti, S. A new mutation in the KIT ATP pocket causes acquired resistance to imatinib in a gastrointestinal stromal tumor patient. *Gastroenterology*, **2004**, *127(1),*294-9.
15. Heinrich, M.C.; Maki, R.G.; Corless, C.L.; Antonescu, C.R.; Harlow, A.; Griffith, D.; Town, A.; McKinley, A.; Ou, W.B.; Fletcher, J.A.; Fletcher, C.D.; Huang, x.; Cohen, D.P.; Baum, C.M.; Demetri, G.D. Primary and secondary kinase genotypes correlate with the biological and clinical activity of sunitinib in imatinib-resistant gastrointestinal stromal tumor. *J. Clin. Oncol.* **2008**, *26*, 5352–5359.
16. Nishida, T.; Takahashi, T.; Nishitani, A.; Doi, T.; Shirao, K.; Komatsu, Y.; Nakajima, K.; Hirota, S. Sunitinib-resistant gastrointestinal stromal tumors harbor cis-mutations in the activation loop of the KIT gene. *Int. J. Clin. Oncol.* **2009**, *14*, 143–149.
17. Demetri, G.D.; van Oosterom, A.T.; Garrett, C.R.; Blackstein, M.E., Shah, M.H., Verweij, J.; McArthur, G.; Judson, I.R.; Heinrich, M.C.; Morgan, J.A.; Desai, J.; Fletcher, C.D.; George, S.; Bello, C.L.; Huang, x.; Baum, C.M.; Casali, P.G. Efficacy and safety of sunitinib in patients with advanced gastrointestinal stromal tumour after failure of imatinib: a randomised controlled trial. *Lancet.* **2006**, *368,*1329–1338.
18. Demetri, G.D.; Reichardt, P.; Kang, Y.K.; Blay, J.Y.; Rutkowski, P.; Gelderblom, H.; Hohenberger, P.; Leahy, M.; von Mehren, M.; Joensuu, H.; Badalamenti, G.; Blackstein, M.; Le Cesne, A.; Schöffski, P.; Maki, R.G.; Bauer, S.; Nguyen, B.B.; xu, J.; Nishida, T.; Chung, J.; Kappeler, C.; Kuss, I.; Laurent, D.; Casali, P.G. Efficacy and safety of regorafenib for advanced gastrointestinal stromal tumours after failure of imatinib and sunitinib (GRID): an international, multicentre, randomised, placebo-controlled, phase 3 trial. *Lancet.* **2013**, *381*, 295–302.
19. Gajiwala, K.S.; Wu, J.C.; Christensen, J.; Deshmukh, G.D.; Diehl, W.; DiNitto, J.P.; English, J.M.; Greig, M.J.; He, Y.A., Jacques SL, Lunney EA, McTigue M, Molina D, Quenzer T, Wells PA, Yu x, Zhang Y, Zou A, Emmett MR, Marshall AG, Zhang HM, Demetri GD. KIT kinase mutants show unique mechanisms of drug resistance to imatinib and sunitinib in gastrointestinal stromal tumor patients. *Proc. Natl. Acad. Sci. U.S.A.* **2009**, *106(5),*1542-7.
20. Jacobson, M.P.; Pincus, D.L.; Rapp, C. S.; Day, T.J.F.; Honig, B.; Shaw, D.E.; Friesner, R.A. A Hierarchical Approach to All-Atom Protein Loop Prediction. *Proteins*, **2004**, *55*, 351-367.
21. Jacobson, M. P.; Friesner, R.A.; xiang, Z.; Honig, B. On the Role of Crystal Packing Forces in Determining Protein Sidechain Conformations. *J. Mol. Biol.* **2002**, *320*, 597-608.
22. Farid, R.; Day, T.; Friesner, R. A.; Pearlstein, R. A. New insights about HERG blockade obtained from protein modeling, potential energy mapping, and docking studies. *Bioorg. & Med. Chem.* **2006**, *14*, 3160-3173.
23. Sherman, W.; Day, T.; Jacobson, M. P.; Friesner, R. A.; Farid, R. Novel Procedure for Modeling Ligand/Receptor Induced Fit Effects. *J. Med. Chem.* **2006**, *49*, 534-553.
24. Sherman, W.; Beard, H. S.; Farid, R. Use of an Induced Fit Receptor Structure in Virtual Screening. *Chem. Biol. Drug Design.* **2006**, *67*, 83-84.

25. Bauer, S.; Joensuu, H. Emerging Agents for the Treatment of Advanced, Imatinib-Resistant Gastrointestinal Stromal Tumors: Current Status and Future Directions. *Drugs*, **2015**, *75*, 1323–1334.
26. Lu, T.; Chen, C.; Wang, A.; Jiang, Z.; Qi, Z.; Hu, Z.; Hu, C.; Liu, F.; Wang, W.; Wu, H.; Wang, B.; Wang, L.; Qi, S.; Wu, J.; Wang, W.; Tang, J.; Yan, H.; Bai, M.; Liu, Q.; Liu, J. Repurposing cabozantinib to GISTs: Overcoming multiple imatinib-resistant cKIT mutations including gatekeeper and activation loop mutants in GISTs preclinical models. *Cancer Lett.,* **2019**, *447*, 105-114.
27. Xie, F.; Xiao, W.; Jiang, Y.; Xia, X. Wang, Y. Relationship between efficacy of sunitinib and KIT mutation of patients with advanced gastrointestinal stromal tumors after failure of imatinib. *Medicine (Baltimore)*, **2019**, *98(19),* e15478.
28. Serrano, C.; Mariño-Enríquez, A.; Tao, D.L.; Ketzer, J.; Eilers, G.; Zhu, M.; Yu, C.; Mannan, A.M.; Rubin, B.P.; Demetri, G.D.; Raut, C.P.; Presnell, A.; McKinley, A.; Heinrich, M.C.; Czaplinski, J.T.; Sicinska, E.; Bauer, S.; George, S.; Fletcher, J.A. Complementary activity of tyrosine kinase inhibitors against secondary kit mutations in imatinib-resistant gastrointestinal stromal tumours. *British Journal of Cancer*, **2019**, *120*, 612–620.
29. Lauria, A.; Mannino, S.; Gentile, C.; Mannino, G.; Martorana, A.M.; Peri, D. DRUDIT, Web-Based DRUgs DIscovery Tools to Design Small Molecules as Modulators of Biological Targets. *Bioinformatics.* **2020**, *36*(5), 1562–1569.
30. DRUDIT: DRUg Discovery Tools. Available online: https://www.drudit.com (accessed on 1° May, 2020).
31. Lauria, A.; Tutone, M.; Almerico, A.M. Virtual lock-and-key approach: the in silico revival of Fischer model by means of molecular descriptors. *Eur. J. Med. Chem.* **2011**, *46(9),* 4274-80.
32. Lauria, A.; Tutone, M.; Barone, G.; Almerico, A.M. Multivariate analysis in the identification of biological targets for designed molecular structures: the BIOTA protocol. *Eur. J. Med. Chem.* **2014**, 21, 75, 106-10.
33. Lauria, A.; Patella, C.; Abbate, I.; Martorana, A.; Almerico, A.M. Lead optimization through VLAK protocol: New annelated pyrrolo-pyrimidine derivatives as antitumor agents. *Eur. J. Med. Chem.* **2012**, *55*, 375-383.
34. Lauria, A.; Abbate, I.; Patella, C.; Martorana, A.; Dattolo, G.; Almerico, A.M. New annelated thieno [2, 3-e][1, 2, 3] triazolo [1, 5-a] pyrimidines, with potent anticancer activity, designed through VLAK protocol. *Eur. J. Med. Chem.* **2013**, *62*, 416-24.
35. BindingDB. Available online: URL: www.bindingdb.org .
36. Lauria. A.; Abbate, I.; Gentile, C.; Angileri, F.; Martorana, A.; Almerico, A.M. Synthesis and biological activities of a new class of heat shock protein 90 inhibitors, designed by energy-based pharmacophore virtual screening. *J. Med. Chem.* **2013**, *56(8),* 3424-8.
37. Bonsignore, R.; Terenzi, A.; Spinello, A.; Martorana, A.; Lauria, A.; Almerico, A.M.; Keppler, B.K.; Barone, G. G-quadruplex vs. duplex-DNA binding of nickel(II) and zinc(II) Schiff base complexes. *J. Inorg. Biochem.* **2016**, *161*, 115-21.
38. Lauria, A.; Alfio, A.; Bonsignore, R.; Gentile, C.; Martorana, A.; Gennaro, G.; Barone, G.; Terenzi, A.; Almerico, A.M. New benzothieno[3,2-d]-1,2,3-triazines with antiproliferative activity: synthesis, spectroscopic studies, and biological activity. *Bioorg. Med. Chem. Lett.* **2014**, *24(15),* 3291-7.
39. Jonathan, B.B.; Holloway, G.A. New Substructure Filters for Removal of Pan Assay Interference Compounds (PAINS) from Screening Libraries and for Their Exclusion in Bioassays. *J. Med. Chem.* **2010**, 53, 7, 2719-2740.

40. Lipinski, C. A.; Lombardo, F.; Dominy, B.W.; Feeney, P.J. Experimental and computational approaches to estimate solubility and permeability in drug discovery and development settings. *Advanced Drug Delivery Reviews*, **2001**, 46, 3-26.
41. Veber, D.F.; Johnson, S.R.; Cheng, H.Y.; Smith, B.R.; Ward, K.W.; Kopple, K.D. Molecular Properties That Influence the Oral Bioavailability of Drug Candidates. *J. Med. Chem.* **2002**, *45*, *12*, 2615-2623.
42. Egan, W.J.; Merz, K.M.; Baldwin, J.J. Prediction of Drug Absorption Using Multivariate Statistics. *J. Med. Chem.* **2000**, *43, 21*, 3867-3877.
43. Daina, A.; Michielin, O.; Zoete, V. SwissADME: a free web tool to evaluate pharmacokinetics, druglikeness and medicinal chemistry friendliness of small molecules. *Nature Scientific Reports,* **2017**, 7, e42717.
44. Schrödinger Release 2017–2, LigPrep, (Schrödinger, LLC, New York, 2017b).
45. Schrödinger Release 2017-2, Schrödinger Suite 2017-2 Protein Preparation Wizard; (Epik, Schrödinger, LLC, New York, 2017a).
46. Banks, J.L.; Beard, H.S.; Cao, Y.; Cho, A.E.; Damm, W.; Farid, R.; Felts, A.K.; Halgren, T.A.; Mainz, D.T.; Maple, J.R.; Murphy, R.; Philipp, D.M.; Repasky, M.P.; Zhang, L.Y.; Berne, B.J.; Friesner, R.A.; Gallicchio, E.; Levy, R.M. Integrated Modeling Program, Applied Chemical Theory (IMPACT). *J. Comput. Chem*. **2005**, *26*, 1752–80.
47. RCSB PDB. Available online: URL www.rcsb.org.
48. Sastry, G.M.; Adzhigirey, M.; Day, T.; Annabhimoju, R.; Sherman, W. Protein and ligand preparation: Parameters, protocols, and influence on virtual screening enrichments. *J. Comput. Aid. Mol. Des*. **2013**, *27(3),* 221-34.
49. Friesner, R. A.; Murphy, R. B.; Repasky, M. P.; Frye, L. L.; Greenwood, J. R.; Halgren,T. A.; Sanschagrin, P. C.; Mainz, D. T. Extra Precision Glide: Docking and Scoring Incorporating a Model of Hydrophobic Enclosure for Protein-Ligand Complexes. *J. Med. Chem.* **2006**, *49*, 6177–96.
50. Halgren, T. A.; Murphy, R. B.; Friesner, R. A.; Beard, H. S.; Frye, L. L.; Pollard, W. T.; Banks, J. L. Glide: A New Approach for Rapid, Accurate Docking and Scoring. 2. Enrichment Factors in Database Screening. *J. Med. Chem*. **2004**, *47*, 1750–9.
51. Friesner, R. A.; Banks, J. L.; Murphy, R. B.; Halgren, T. A.; Klicic, J. J.; Mainz, D. T.; Repasky, M. P.; Knoll, E. H.; Shaw, D. E.; Shelley, M.; Perry, J. K.; Francis, P.; Shenkin, P. S. Glide: A New Approach for Rapid, Accurate Docking and Scoring. 1. Method and Assessment of Docking Accuracy. *J. Med. Chem*. **2004**, *47*, 1739–49.
52. Sherman, W.; Day, T.; Jacobson, M. P.; Friesner, R. A.; Farid, R. Novel Procedure for Modeling Ligand/Receptor Induced Fit Effects. *J. Med. Chem.* **2006**, *49*, 534-53.
53. Sherman, W.; Beard, H. S.; Farid, R. Use of an Induced Fit Receptor Structure in Virtual Screening. *Chem. Biol.Drug Design*. **2006**, *67*, 83-84.
54. Maestro, version 9.3, Schrödinger, LLC, New York, NY, **2012**.
55. Zhong, H.; Tran, L.M.; Stang, J.L. Induced-fit docking studies of the active and inactive states of protein tyrosine kinases. *J. Mol. Graph. Model*. **2009**, *28*, 336–46.
56. Wanga, H. Induced-fit docking of mometasone furoate and further evidence for glucocorticoid receptor 17α pocket flexibility. *J. Mol. Graph. Model.* **2008**, 27, 512–521.
57. Luo, H.J.; Wang, J.Z.; Deng, W.Q.; Zou, K. Induced-fit docking and binding free energy calculation on furostanol saponins from Tupistra chinensis as epidermal growth factor receptor inhibitors. *Med. Chem. Res*. **2013**, *22*, 4970–9.
58. Jacobson, M. P.; Pincus, D. L.; Rapp, C. S.; Day, T. J. F.; Honig, B.; Shaw, D. E.; Friesner, R. A. A Hierarchical Approach to All-Atom Protein Loop Prediction. *Proteins*. **2004**, *55*, 351-67.

59. Jacobson, M. P.; Friesner, R.A.; xiang, Z.; Honig, B. On the Role of Crystal Packing Forces in Determining Protein Sidechain Conformations. *J. Mol. Biol.* **2002**, *320*, 597-608.